


# Thermally Driven Ionic Aggregation in Poly(ethylene oxide)-Based Sulfonate Ionomers

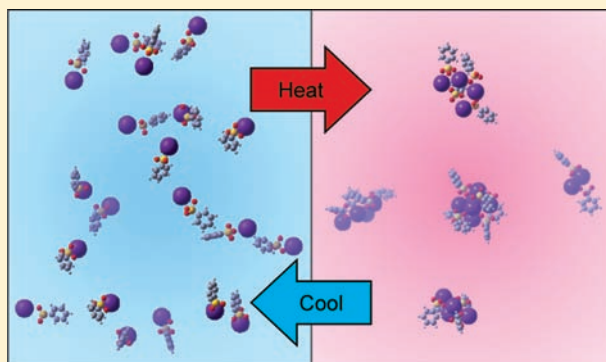
Wenqin Wang,<sup>‡,§</sup> Gregory J. Tudryn,<sup>†</sup> Ralph H. Colby,<sup>†</sup> and Karen I. Winey<sup>\*‡</sup>

<sup>‡</sup>Department of Materials Science and Engineering, University of Pennsylvania, Philadelphia, Pennsylvania 19104-6272, United States

<sup>†</sup>Department of Materials Science and Engineering and Materials Research Institute, Pennsylvania State University, University Park, Pennsylvania 16802, United States

 Supporting Information

**ABSTRACT:** A series of sulfonate polyester ionomers with well-defined poly(ethylene oxide) spacer lengths between phthalates and alkali metal cations as counterions are designed for improved ionic conductivity. Ion conduction in these chemically complex materials is dominated by the polymer mobility and the state of ionic aggregation. While the aggregation decreases dramatically at room temperature as the cation size increases from Li to Na to Cs, the extents of ionic aggregation of these ionomers are comparable at elevated temperatures. Both the Na and Cs ionomers exhibit thermally reversible transformation upon heating from 25 to 120 °C as isolated ion pairs aggregate. This seemingly counterintuitive aggregation of ions on heating is driven by the fact that the dielectric constant of all polar liquids decreases on heating, enhancing Coulomb interactions between ions.



## INTRODUCTION

Poly(ethylene oxide) (PEO) with dissolved salt is a common polymer electrolyte. The high ion conductivity in these PEO/salt mixtures arises from both the good solubility of salts in this polymer<sup>1–4</sup> and the low glass transition temperature of PEO, as ion mobility in polymer electrolytes is strongly coupled with the segmental motion of the polymer chain.<sup>5,6</sup> However, these bi-ion conductors typically exhibit anion buildup at the electrode/electrolyte interface that ultimately lowers the effective field on the cations and raises the applied field required to transport cations, limiting their applicability in batteries and other devices. In contrast, ionomers with anions fixed to the polymer backbone are single-ion conductors that avert the concentration polarization problem, and their ion conductivity is highly dependent on the association states of the ionic groups.

Historically, ion conductivity in ionomers with metal counterions has been considerably lower than that in PEO/salt mixtures, because the low dielectric constant of the ionomers promotes microphase separation of the ions (called ionic aggregation).<sup>7</sup> To minimize ionic aggregation and thereby enhance ion conductivity, we recently synthesized a series of PEO–sulfonate polyester ionomers using a step growth reaction between poly(ethylene glycol) (PEG) diols of well-defined molecular weight and dimethyl *S*-sulfoisophthalate sodium salt.<sup>8</sup> After polymerization, the Na<sup>+</sup> counterion can be fully exchanged with Li<sup>+</sup> or Cs<sup>+</sup> during the aqueous dialysis used for purification. These PEO-based ionomers are denoted as PEO<sub>*x*</sub>–*y*%M, where

*x* is the molecular weight of PEO spacers in g/mol (400, 600, or 1100), *y* is the percent of phthalates that are sulfonated in the ionomers (in this paper either 0 or 100%), and M denotes the cation (Li, Na, or Cs). The nonionic polyesters (PEO<sub>*x*</sub>–0%) were made from dimethyl isophthalate and PEG for comparison. Insets in Figure 1 (below) show the chemical structures for various PEO600 materials.

We previously reported the room-temperature morphology of these PEO–sulfonate polyester ionomers as a function of PEO segment length and alkali cation type (Li, Na, and Cs).<sup>9</sup> These prior results are summarized here to provide an important foundation for understanding the unexpected temperature-dependent findings reported in the present paper. The PEO–sulfonate polyester ionomers exhibit hierarchical structures at room temperature that were probed primarily by X-ray scattering over a wide range of scattering angles corresponding to spacings of 0.3–70 nm. The nature of these hierarchical morphologies depends on both the length of the PEO spacer and the cation type. When the PEO spacer has a molecular weight of 1100 g/mol or higher, the PEO segments crystallize at room temperature, as evidenced by X-ray scattering peaks consistent with PEO crystallites and a lamellar morphology at high and low scattering angles, respectively. Moreover, the thicknesses of the lamellae are

Received: February 14, 2011

Published: June 24, 2011

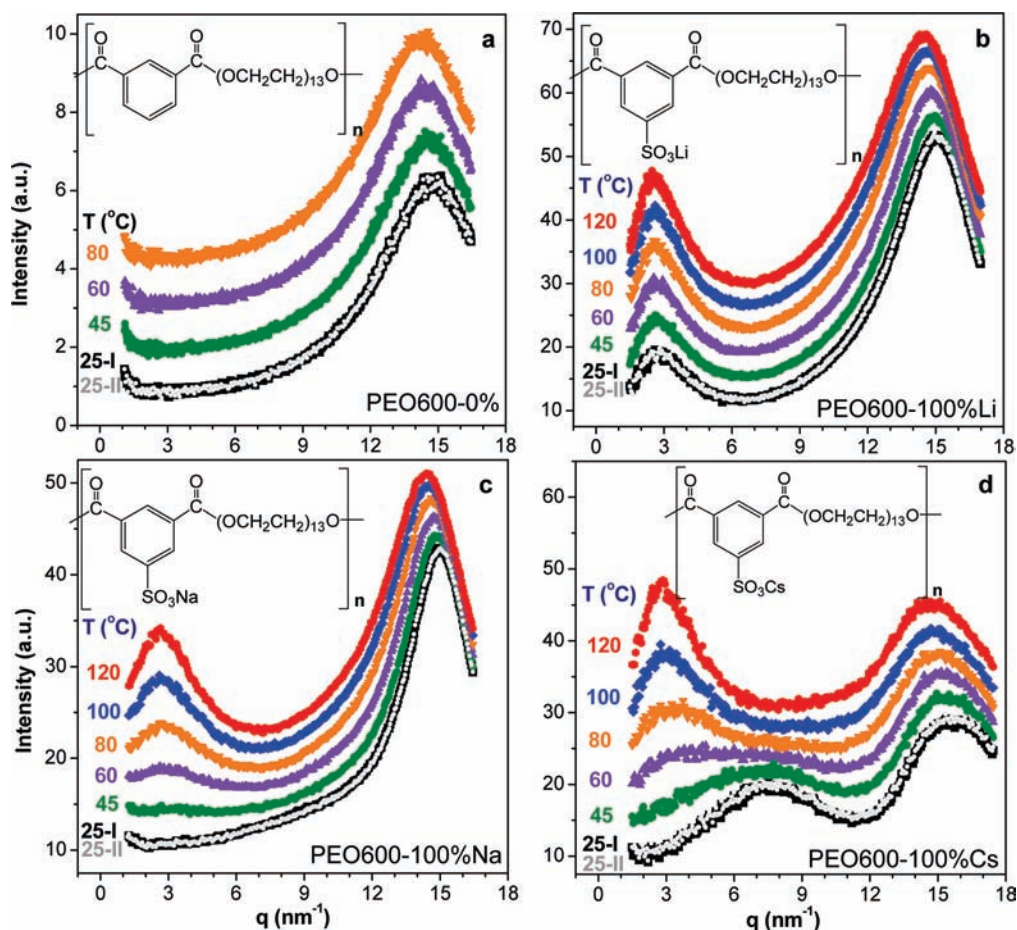


**Figure 1.** X-ray scattering data of (a) PEO600–0%, (b) PEO600–100% Li, (c) PEO600–100% Na, and (d) PEO600–100% Cs, each at six temperatures. The scattering data at higher temperatures were vertically shifted for clarity. The identical patterns at 25 °C before (black, 25-I) and after (gray, 25-II) heating indicate that all changes in scattering are thermally reversible.

well-defined (as indicated by higher order scattering reflections) and correspond to the molecular weight of the PEO spacer.

Of greater relevance to this paper is the state of ionic aggregation of the amorphous PEO–sulfonate polyester ionomers as a function of cation type.<sup>9</sup> The Li-neutralized PEO-based ionomers exhibit the widely reported ionomer morphology of ionic aggregates at room temperature. Two pieces of scattering data contribute to this conclusion. A scattering peak at  $2.7 \text{ nm}^{-1}$  arises from an interaggregate spacing of  $\sim 2.3 \text{ nm}$ . This is the traditional “ionomer peak” and is detectable in these Li-neutralized ionomers, despite the low electron density contrast, because monodisperse PEO spacer length separates ions at regular intervals along the polymer molecule.<sup>9,10</sup> Second, a scattering peak persists at  $15.0 \text{ nm}^{-1}$  after subtraction of the scattering from a nonionic PEO–sulfonate polymer that is consistent with the interatomic distances calculated for Li quadrupoles ( $\text{SO}_3^- \text{Li}^+$ )<sub>2</sub> in benzene sulfonate. The local structure of quadrupoles is consistent with ionic aggregates.

In contrast, at room temperature the ions in Cs-neutralized PEO-based ionomers exist as isolated ion pairs ( $\text{SO}_3^- \text{Cs}^+$ ).<sup>9</sup> Evidence for ion pairs comes from the high scattering angle regime, where after subtraction of the nonionic PEO-based polymer the Cs-neutralized PEO–sulfonate polyester ionomers exhibit a peak at  $17.4 \text{ nm}^{-1}$ , which corresponds to the interatomic distances in ion pairs. Furthermore, these Cs ionomers

have a scattering peak at  $\sim 7 \text{ nm}^{-1}$  which is higher  $q$  than the peak position for a traditional ionomer peak and corresponds to a correlation distance of just  $0.9 \text{ nm}$ . Using the number of ion pairs from the stoichiometry of the polymer and the polymer density, the correlation distance between isolated ion pairs is  $\sim 1.1 \text{ nm}$ . Thus, we concluded that the majority of ions exist as isolated ion pairs. Given that Cs-neutralized polystyrene-based ionomers do exhibit a traditional ionomer peak, it is the combination of the large cation and the relatively high dielectric constant matrix that produces this morphology of isolated ion pairs in Cs-neutralized PEO-based ionomers. Finally, we found that the Na-neutralized PEO–sulfonate polyester ionomers exhibit a state of ionic aggregation that is intermediate between isolated ion pairs and ionic aggregates.<sup>9</sup> The cation-specific morphologies were consistently observed for all three of the PEO spacer lengths studied.

In this paper we present evidence for a thermally reversible transformation in the extent of ionic aggregation in PEO-based ionomers. At room temperature, only the ionomers with  $\text{Li}^+$  counterions exhibit well-defined ionic aggregates, while at elevated temperatures ionomers with  $\text{Li}^+$ ,  $\text{Na}^+$ , and  $\text{Cs}^+$  counterions all form ionic aggregates. This transformation is driven by the decrease in dielectric constant as temperature is raised,<sup>11</sup> enhancing the Coulomb interactions between ions, and provides new understanding upon which to design improved polymer electrolytes.

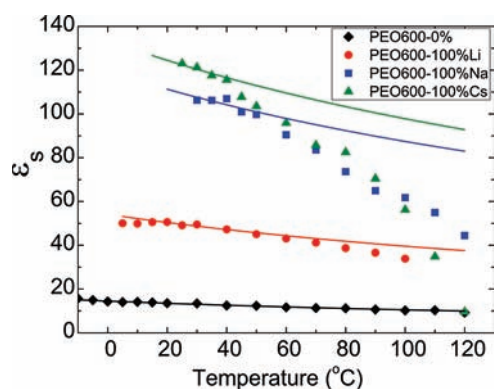


**Figure 2.** Temperature dependence of static (low-frequency) dielectric constants of PEO600–0% (black diamond), PEO600–100% Li (red circles), PEO600–100% Na (blue squares), and PEO600–100% Cs (green triangles). The solid curves are the Onsager equation with fixed concentration and dipole of polar groups. The black curve is eq 1 with  $\Sigma_i \nu_i m_i^2 / 9\epsilon_0 k = 418$  K for the dipoles in the PEO600–0% nonionic polyester. The colored curves are eq 2 with  $\nu_{\text{pair}} m_{\text{pair}}^2 / 9\epsilon_0 k = 1290$  K for PEO600–100% Li (red), 3400 K for PEO600–100% Na (blue), and 3850 K for PEO600–100% Cs (green), assuming the dipoles of the nonionic polymer make the same contribution to the dielectric constants of the ionomers.

## EXPERIMENTAL SECTION

**Materials.** Poly(ethylene oxide)-based ionomers were prepared by a two-step melt polycondensation as detailed previously.<sup>8</sup> Poly(ethylene glycol) diols of different molecular weights were reacted with either dimethyl 5-sulfoisophthalate sodium salt or dimethyl isophthalate to prepare ionomers and nonionic polyesters, respectively. <sup>1</sup>H NMR verified the chemical structures as shown in the insets in Figure 1. The molecular weights of these ionomers range from 3000 to 6000 g/mol, as published previously.<sup>9</sup> The molecular weights of PEO spacers are 400, 600, or 1100 g/mol, which were determined by <sup>1</sup>H NMR of the PEG diols. The cation was exchanged from sodium to lithium or cesium by aqueous diafiltration with an excess of LiCl or CsCl salts, then exhaustively dialyzed to remove salt impurities.<sup>8</sup> The concentrated ionomer solutions were freeze-dried after diafiltration and then vacuum-dried at 120 °C to constant mass.

**X-ray Scattering.** To minimize the exposure of the materials to moisture, previously dried materials were loaded into the capillaries under vacuum at elevated temperatures (70–110 °C, depending on the viscosity of the ionomers). As the samples flow into the capillary under vacuum, bubbles were eliminated. The filled capillaries were cooled to room temperature under vacuum and then quickly flame-sealed for X-ray scattering experiments. Alternatively, capillaries loaded with high-viscosity ionomers were kept open at both ends and stored under vacuum. Temperature scans were performed in the Multiple Angle X-ray Scattering facility at the University of Pennsylvania from room temperature to 120 °C with a step size of ~20 K and a heating and cooling rate of 10 K/min. The samples were equilibrated at each temperature for 10 min before starting the X-ray data collection; typical data collection times were 60 min/sample. Note that these ionomers have very low  $T_g$  (<25 °C) and relatively low molecular weight,<sup>9</sup> so they are able to reach thermodynamic equilibrium rapidly. Previous rheological studies have showed that the terminal relaxation time of these materials is ~1 s or less at 30 °C.<sup>8</sup>

The multiangle X-ray scattering system used Cu K $\alpha$  X-ray from a Nonius FR 591 rotating-anode generator operated at 40 kV and 85 mA. The bright, highly collimated beam was obtained via Osmic Max-Flux optics and triple-pinhole collimation under vacuum. The scattering data were collected using a Bruker Hi-Star multiwire detector with sample-to-detector distances of 11 and 54 cm. The 2-D data reduction and analysis

were performed using Datasqueeze software.<sup>12</sup> Background scattering from an empty capillary was subtracted from the samples' scattering.

**Dielectric Relaxation Spectroscopy.** A Novocontrol GmbH Concept 40 broadband dielectric spectrometer was used to measure the frequency-dependent dielectric permittivity. Samples were placed on a polished brass electrode and dried in a vacuum oven at 80 °C for at least 24 h, after which a second polished brass electrode was placed on top with 50  $\mu\text{m}$  silica spacers used to control sample thickness and returned to heated vacuum for at least 12hrs for further drying. To minimize effects of water, each sample was held at 120 °C for 1 h in the instrument prior to measurements; Karl Fischer titration after analysis suggests the water content of our samples is less than 20 ppm. Frequency sweeps were performed from 10 MHz to 0.01 Hz at each temperature studied. The static dielectric constants plotted in Figure 2 are taken as the low-frequency limit of permittivity before the onset of electrode polarization starts.

## RESULTS AND DISCUSSION

Figure 1 shows the variable-temperature X-ray scattering of PEO600–100% Li, Na, and Cs, as well as the nonionic polyester PEO600–0%. The room-temperature X-ray scattering results illustrate the morphologies summarized above. Although PEO is a semicrystalline homopolymer, these ionomers are amorphous because the PEO spacer is short (600 g/mol corresponds to 13  $-\text{CH}_2\text{CH}_2\text{O}-$  repeat units), and when PEO spacer length is 1100 g/mol our thermal treatment prevents crystallization. The absence of crystallinity permits us to focus on ionic aggregation. All the morphology transformations that occur upon heating from 25 to 120 °C are fully reversible in all of the materials, as exemplified by the identical scattering patterns at 25 °C before and after heating. In addition, selected materials were thermally cycled several times, and the observed scattering patterns at different temperatures are independent of cycle number.

The only morphological change upon heating the nonionic polymer, PEO600–0%, to 120 °C is a slight shift to lower  $q$  in the amorphous halo ( $q \approx 15 \text{ nm}^{-1}$ ) corresponding to thermal expansion (Figure 1a); this peak shift is observed in all of the polymers. The scattering peak ( $q \approx 2.6 \text{ nm}^{-1}$ ) associated with ionic aggregates in PEO600–100% Li persists at all temperatures (Figure 1b), indicating that the ionic aggregates are thermally stable up to 120 °C. Similarly, the ionic aggregates in PEO400–100% Li (Supporting Information (SI), Figure S1) and PEO1100–100% Li (SI, Figure S2) persist up to 120 °C. This is the expected and widely reported finding in ionomers,<sup>7</sup> wherein the enthalpic driving forces for ionic aggregation dominate the ionomer morphology and the attractions between ion pairs are stable to temperatures above the thermal degradation of the polymer.

In contrast, both PEO600–100% Na and PEO600–100% Cs develop ionic aggregates upon heating (Figure 1c,d). The ionomers with Na<sup>+</sup> counterions at room temperature have a variety of local ion-pair environments that upon heating transform into well-defined ionic aggregates, as evidenced by the emerging peak at  $q \approx 2.8 \text{ nm}^{-1}$ . Scattering peaks associated with ionic aggregates also arise in PEO400–100% Na (SI, Figure S3) and PEO1100–100% Na (SI, Figure S4). The morphologies of PEO600–0% and PEO600–100% Na were also probed over a broader angular range ( $0.03 < q < 10 \text{ nm}^{-1}$ ) at Argonne National Laboratory at 25, 50, and 100 °C (SI, Figure S5). While the scattering patterns are unresponsive to temperature below  $q \approx 1 \text{ nm}^{-1}$ , the results above  $q \approx 1 \text{ nm}^{-1}$  are consistent with Figure 1a,c. This onset of ionic aggregates is further supported by recent findings from an infrared spectroscopic study of the



same PEO600–100% Na ionomer.<sup>13</sup> Analysis of the  $\text{SO}_3^-$  symmetric stretching band showed that the relative population of aggregated  $\text{SO}_3^-$ , which vibrate as  $2\text{Na}^+(\text{SO}_3^-)$ , increases with increasing temperature, indicating an increasing extent of ionic aggregation.<sup>13</sup>

Upon heating the ionomers with  $\text{Cs}^+$  counterions, the scattering peak at  $q \approx 7 \text{ nm}^{-1}$ , corresponding to interpair scattering from isolated ion pairs at room temperature decreases in intensity as a new scattering peak develops at  $q \approx 3.0 \text{ nm}^{-1}$ . This new peak corresponds to interaggregate scattering from ionic aggregates. Ionic aggregates also emerged at elevated temperatures in PEO400–100% Cs (SI, Figure S6) and PEO1100–100% Cs (SI, Figure S7). At 60 and 80 °C, contributions from both the isolated ion pairs and the ionic aggregates are evident in PEO600–100% Cs (Figure 1d), indicating that regions of primarily isolated ion pairs coexist with regions of primarily ionic aggregates containing multiple ion pairs. This coexistence of isolated ion pairs and ionic aggregates is even more clearly seen in PEO1100–100% Cs at 60, 80, and 100 °C (Figure S7).

Thermally reversible transformations in ionomers from nonaggregated states to aggregated states upon heating are unprecedented in the literature. Previous X-ray scattering studies have reported nonreversible, thermally driven transformations in ionomers that can largely be attributed to the elimination of solvent and thermal equilibration.<sup>14–16</sup> The conventional view of an ionic aggregate is a nanosize ionic assembly that might dissociate at sufficiently high temperature,<sup>7</sup> which provides no insight toward understanding our observation of aggregation of ion pairs as temperature is raised. What does help us understand aggregation on heating is the fact that the dielectric constant,  $\epsilon_s$ , of any polar liquid decreases on heating due to thermal randomization of dipoles.<sup>11</sup> With  $\epsilon_s$  in the denominator of the Coulomb energy, ionic interactions become more dominant upon heating. Hence, we next consider the dielectric constant of these PEO-based ionomers as measured by dielectric relaxation (impedance) spectroscopy.

The temperature dependences of the dielectric constant for the four polymers in Figure 1 are shown in Figure 2. The non-ionic polyester PEO600–0% shows exactly the temperature dependence expected for any polar liquid with fixed concentrations and strengths of dipoles, given by the Onsager equation:<sup>11</sup>

$$\left[ \frac{(\epsilon_s - \epsilon_\infty)(2\epsilon_s + \epsilon_\infty)}{\epsilon_s(\epsilon_\infty + 2)^2} \right]_{\text{nonionic}} = \frac{1}{9\epsilon_0 kT} \sum_i \nu_i m_i^2 \quad (1)$$

where  $\epsilon_s$  is the static (low-frequency) dielectric constant of the liquid and  $\epsilon_\infty$  is the high-frequency dielectric constant (here taken to be the square of the refractive index of PEO),  $\epsilon_0$  is the permittivity of vacuum,  $k$  is the Boltzmann constant,  $T$  is absolute temperature, and  $\nu_i$  are the number densities and  $m_i$  the strengths of the dipoles in the liquid. The solid black curve in Figure 2 is eq 1 with the  $\sum_i \nu_i m_i^2$  term as a constant adjusted to fit the data for PEG600–0%, showing that the nonionic polyester is a simple polar liquid. Since the ionomers have polar ester and ether groups identical to those in the nonionic polyester, we can analyze the dielectric constant of the ionomers to focus on the effects of ions by simple addition.<sup>17</sup>

$$\left[ \frac{(\epsilon_s - \epsilon_\infty)(2\epsilon_s + \epsilon_\infty)}{\epsilon_s(\epsilon_\infty + 2)^2} \right]_{\text{ionomer}} = \frac{\nu_{\text{pair}} m_{\text{pair}}^2}{9\epsilon_0 kT} + \left[ \frac{(\epsilon_s - \epsilon_\infty)(2\epsilon_s + \epsilon_\infty)}{\epsilon_s(\epsilon_\infty + 2)^2} \right]_{\text{nonionic}} \quad (2)$$

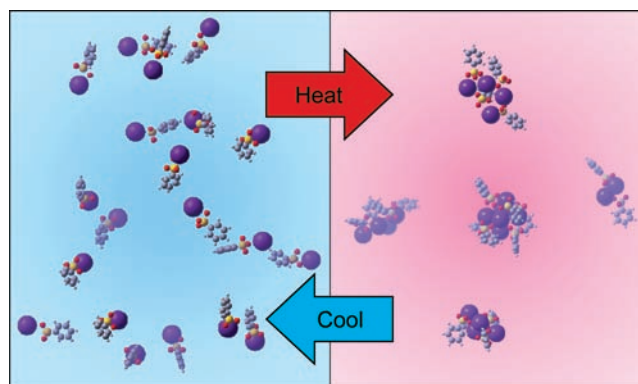


**Figure 3.** Schematic showing the  $\text{SO}_3^- \text{Cs}^+$  ion pairs in PEO $x$ –100% Cs ionomers that reversibly transform between isolated ion pairs and ionic aggregates. At low temperature the isolated ion pairs have an average correlation distance between ion pairs of  $\sim 0.9 \text{ nm}$  (X-ray scattering maximum at  $\sim 7 \text{ nm}^{-1}$ ). At elevated temperatures the  $\text{SO}_3^- \text{Cs}^+$  ion pairs aggregate to form traditional ionic aggregates with an interaggregate separation of  $\sim 2.1 \text{ nm}$  (X-ray scattering maximum at  $\sim 3.0 \text{ nm}^{-1}$ ).

This approach allows the number density of ion pairs  $\nu_{\text{pair}}$  and/or their dipole strength  $m_{\text{pair}}$  to be studied. Equation 2 is fit to the near-room temperature data of each ionomer, effectively adjusting  $\nu_{\text{pair}} m_{\text{pair}}^2$  as a constant fitting parameter (solid colored curves in Figure 2). For each ionomer, eq 2 fits well at low temperature, describing the decrease in dielectric constant as temperature increases. However, when the dielectric constant becomes small enough such that ion pairs start to aggregate, the dielectric constant decreases more rapidly as temperature increases because isolated ion pairs are effectively removed from the liquid. For the Li ionomer, the extra decrease in dielectric constant is subtle, consistent with Figure 1b exhibiting a modest additional aggregation of ion pairs on heating to 120 °C. However, for the Na and Cs ionomers, the deviation from eq 2 with constant  $\nu_{\text{pair}} m_{\text{pair}}^2$  is striking and consistent with the obvious increases in aggregation of ion pairs seen in Figure 1c,d. Consequently, we attribute the aggregation on heating in our ionomers to a stronger Coulomb interaction as the dielectric constant decreases. This enhanced aggregation, of course, makes the dielectric constant decrease even more rapidly, causing further aggregation as  $T$  is raised. Since all ionomers above their glass transition are polar liquids, we expect aggregation of ions upon heating to be an important universal feature of this class of materials. Figure 3 schematically shows ion pairs well-separated at low temperature to represent isolated ion pairs and aggregated ion pairs at elevated temperature. The schematic was constructed using previously reported *ab initio* calculations of cesium benzene sulfonate.<sup>9</sup>

Similar aggregation of ions on heating has been observed in mixtures of polyethers with salts or neutralized acid copolymers.<sup>18–23</sup> For example, a Raman spectroscopic study of a poly(propylene oxide)/ $\text{NaCF}_3\text{SO}_3$  mixture showed that the amount of dissociated free ions decreases with increasing temperature in an Arrhenius fashion.<sup>19</sup> Increasing temperature resulted in ion pairing in polyether/salt mixtures.<sup>19</sup> In some cases, salt precipitation in polyether/salt mixtures was observed as the temperature increased.<sup>18,22,24</sup> In blends of PEG with partially Li-neutralized poly(acrylic acid) ionomers, a lower critical solution temperature was observed, which was attributed to weakening intermolecular interactions.<sup>23</sup> These various studies are consistent with our

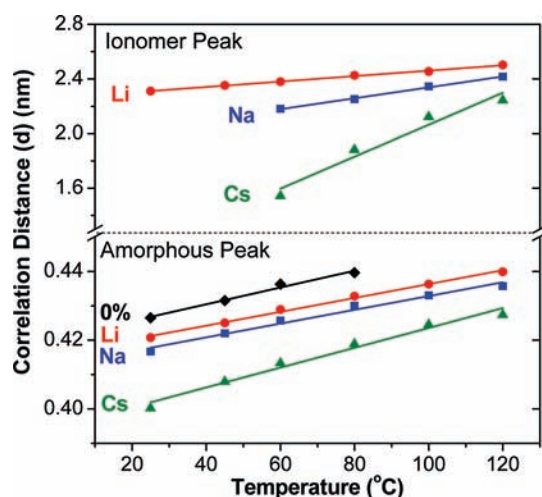


**Figure 4.** Temperature dependence of correlation distance ( $d = 2\pi/q^*$ ) of amorphous peaks in PEO600–0% (black diamonds) and PEO600–100% M and ionomer peaks in PEO600–100% M, with M = Li (red circles), Na (blue squares), and Cs (green triangles).

findings in PEO-based ionomer systems and could be attributed to phase separation driven by the decrease in dielectric constant that accompanies increasing temperature. In the remainder of this paper we discuss additional X-ray scattering data to support our finding that increasing temperature drives ionic aggregation in PEO-based ionomers.

The intensity and peak position of the scattering peak for ionic aggregates indicate that the nature of the ionic aggregates evolves with increasing temperature for all cations, although the extent of this transformation depends on the cation type. For comparison, consider the scattering peak from the amorphous PEO spacer at  $q \approx 15 \text{ nm}^{-1}$  that shows little change in intensity and only a modest shift to lower  $q$ , as expected for thermal expansion in the absence of changes in composition. In contrast, the scattering peak from the ionic aggregates changes significantly in both intensity and peak position. The ionomer peak intensity arises from both the uniformity of the interaggregate spacing and the electron density difference between the matrix and the ionic aggregate. For the Li ionomers the increase in ionomer peak intensity (Figures 1b, S1, and S2) suggests that the ionic aggregates are becoming more ionic, perhaps by releasing ether oxygens trapped within the ionic aggregates at lower temperatures. In addition, less thermal expansion within the ionic aggregates due to stronger secondary bonding than in the PEO matrix can also contribute to increases in electron density differences and thereby increases in ionomer peak intensity.

Regarding peak position, Figure 4 shows the characteristic lengths of the ionomer peak and amorphous halo, corresponding to the interaggregate separation and the interchain spacing, respectively, as functions of temperature for all the PEO600 polymers. The rate of increase in interchain separation is comparable for all the cations, while interaggregate spacings change significantly faster, with the Cs ionomer changing the fastest of all. Given that the volume fraction of ionic groups within a polymer is fixed, any transformation from isolated ion pairs to ionic aggregates that contain multiple ion pairs requires the correlation distance to increase. Similar trends in peak position exist in PEO400 and PEO1100 ionomers (SI, Figure S8).

The X-ray scattering data of PEO $x$ –100% Na ( $x = 400, 600,$  and 1100) at 120 °C are shown in Figure 5a. The ionomer peak

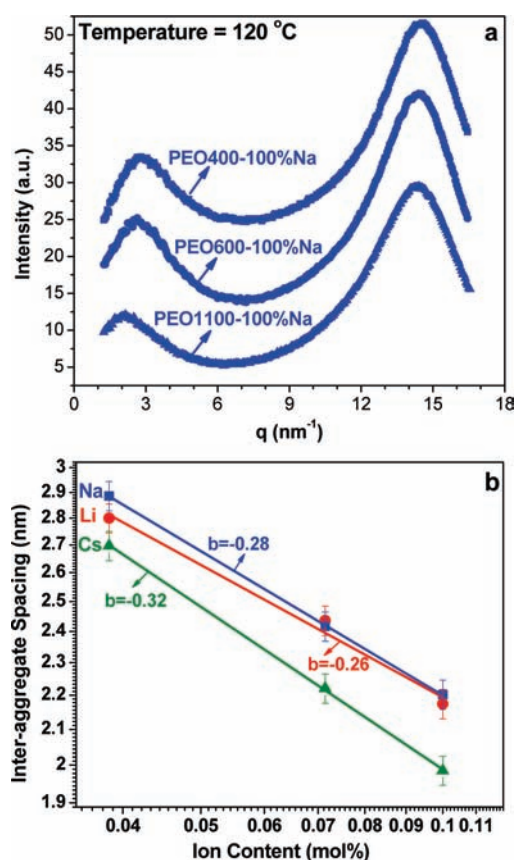


**Figure 5.** (a) X-ray scattering data of PEO $x$ –100% Na ( $x = 400, 600,$  and 1100 g/mol) at 120 °C. The ionomer peak position ( $q = 2-3 \text{ nm}^{-1}$ ) in PEO $x$ –100% Na at 120 °C shifts to a higher scattering wavevector as  $x$  decreases because the ion content increases. (b) Average interaggregate spacing ( $d$ ) obtained from the ionomer peak position ( $d = 2\pi/q^*$ ) at 120 °C in PEO $x$ –100% M (M = Li, red circles; Na, blue squares; and Cs, green triangles), which follows a power law dependence on the ion content ( $C$ ):  $d \sim C^b$ , where  $b = -0.26, -0.28,$  and  $-0.32$  for Li, Na, and Cs, respectively. The lines are the best fit of the data with the allometric function ( $d \sim C^b$ ).

increases in intensity and shifts to higher  $q$  as the PEO spacer length decreases, that is, as the ion content increases, as expected when the ionomer peak arises from the interaggregate spacing.<sup>25–30</sup> The average interaggregate spacing ( $d$ ) obtained from the ionomer peak position ( $d = 2\pi/q^*$ ) at 120 °C in PEO $x$ –100% M follows a power law dependence with the ion content ( $C$ ):  $d \sim C^b$ , where  $b = -0.26, -0.28,$  and  $-0.32$  for Li, Na, and Cs ionomers, respectively (Figure 5b). When ionic aggregates are discrete and uniform in size, with a constant number of ion pairs per aggregate and a constant fraction of ion pairs in aggregates, the predicted scaling law with increasing ion content has an exponent  $b = -1/3$ . This prediction is comparable to the observed values for these PEO-based ionomers and thereby suggests that the ionic aggregates at 120 °C are independent of the PEO spacer length. Ionomers with regular spacing between ionic groups, such as carboxy-telechelic polyisoprenes<sup>31</sup> and sulfonated polyurethanes,<sup>32</sup> have previously shown a  $-1/3$  power law relationship within experimental error.<sup>33</sup> In contrast, random ionomers show a much weaker dependence on the ion content,<sup>14,33</sup> with  $b = -0.1$  to  $-0.2$ . Our observation that the same ionic aggregates are found regardless of PEO spacer length

is further evidence that temperature, and thereby dielectric constant, rather than PEO spacer length, controls the extent of aggregation. Until direct imaging experiments of the nanoscale ionic aggregates in the low- $T_g$  ionomers determine the shape of the ionic aggregates as a function of cation type, further analyses of the X-ray scattering results are limited.

## CONCLUSIONS

Ion conductivity in ionomers is acutely sensitive to the local environment of the ions. In PEO-based ionomers with well-defined PEO spacers, our X-ray scattering and dielectric spectroscopy show that aggregation of the ion pairs increases with increasing temperature. This is more pronounced in ionomers with large cations, specifically Cs ionomers, which transform from having isolated ion pairs below 40 °C to ionic aggregates at 120 °C. The Na ionomers transition from a variety of local environments at room temperature to well-defined ionic aggregates at 120 °C. Even the Li ionomers that exhibit ionic aggregates at room temperature show signs of somewhat increased ionic aggregation as the ionomer scattering peak intensity increases upon heating. Dielectric measurements also find that the extent of ionic aggregation increases most significantly for the Cs ionomers. Furthermore, the interaggregate spacing decreases with increasing ion content with a  $-1/3$  power law at 120 °C, showing that the PEO spacer length has little impact on the extent of ionic aggregation. Ion aggregation is fully reversible and intimately connected to the temperature dependence of the dielectric constant. Although the morphologies of our PEO-sulfonate polyester ionomers are greatly affected by the cation type at room temperature, these ionomers exhibit strong ionic aggregation at 120 °C, independent of cation type. The ionic conductivity of these PEO-based ionomers is low, due to the fact that most of the ions form bound states, either ion pairs or aggregates, with an extremely low concentration of conducting (free or positive triple) ions.<sup>17,34</sup> The conductivity of these ionomers increases with temperature, because of the increases in both conducting ion concentration and their mobility with temperature.<sup>34</sup> The temperature dependence of conducting ion concentration in both Na- and Cs-neutralized ionomers deviates from Arrhenius behavior, indicating that there might be multiple activation energies due to the change in ionic association behavior.<sup>34</sup> This is consistent with our X-ray scattering results.

## ASSOCIATED CONTENT

**Supporting Information.** Variable-temperature X-ray scattering data from six additional PEO $_x$ -100% M ionomers, where  $x = 400$  and  $1100$  and  $M = \text{Li}, \text{Na},$  and  $\text{Cs}$ ; variable-temperature ultra-small-angle X-ray scattering data from PEO600-0% and PEO600-100% Na (USAXS performed at the Advanced Photon Source at Argonne National Laboratory). This material is available free of charge via the Internet at <http://pubs.acs.org>.

## AUTHOR INFORMATION

**Corresponding Author**  
winey@seas.upenn.edu

### Present Address

<sup>5</sup>The Dow Chemical Co., 727 Norristown Rd., Spring House, PA 19477

## ACKNOWLEDGMENT

This work is supported by the Department of Energy, Office of Basic Energy Sciences, under Grant No. DE-FG02-07ER46409. Use of the Advanced Photon Source at Argonne National Laboratory was supported by the U.S. Department of Energy, Office of Science, Office of Basic Energy Sciences, under Contract No. DE-AC02-06CH11357. The authors gratefully acknowledge Shichen Dou for synthesis and Wenjuan Liu for generating the graphics for Figure 3. We also thank Janna K. Maranas, Scott T. Milner, Karl T. Mueller, Michael Rubinstein, James Runt, and Michelle E. Seitz for helpful discussions.

## REFERENCES

- (1) Xu, K. *Chem. Rev.* **2004**, *104*, 4303–4417.
- (2) Wright, P. V. *Br. Polym. J.* **1975**, *7*, 319–327.
- (3) Tarascon, J. M.; Armand, M. *Nature* **2001**, *414*, 359–367.
- (4) Armand, M.; Tarascon, J. M. *Nature* **2008**, *451*, 652–657.
- (5) Meyer, W. H. *Adv. Mater.* **1998**, *10*, 439–448.
- (6) Ratner, M. A. In *Polymer Electrolyte Reviews*; MacCallum, J. R., Vincent, C. A., Eds.; Elsevier: New York, 1987; Vol. 1.
- (7) Eisenberg, A.; Kim, J.-S. *Introduction to Ionomers*; John Wiley & Sons: New York, 1998.
- (8) Dou, S. C.; Zhang, S. H.; Klein, R. J.; Runt, J.; Colby, R. H. *Chem. Mater.* **2006**, *18*, 4288–4295.
- (9) Wang, W.; Liu, W.; Tudryn, G. J.; Colby, R. H.; Winey, K. I. *Macromolecules* **2010**, *43*, 4223–4229.
- (10) Seitz, M. E.; Chan, C. D.; Opper, K. L.; Baughman, T. W.; Wagener, K. B.; Winey, K. I. *J. Am. Chem. Soc.* **2010**, *132*, 8165–8174.
- (11) Onsager, L. *J. Am. Chem. Soc.* **1936**, *58*, 1486–1493.
- (12) Heiney, P. A. *Commission on Powder Diffraction Newsl.* **2005**, *32*, 9–11.
- (13) Lu, M.; Runt, J.; Painter, P. *Macromolecules* **2009**, *42*, 6581–6587.
- (14) Weiss, R. A.; Lefelar, J. A. *Polymer* **1986**, *27*, 3–10.
- (15) Register, R. A.; Sen, A.; Weiss, R. A.; Cooper, S. L. *Macromolecules* **1989**, *22*, 2224–2229.
- (16) Benetatos, N. M.; Winey, K. I. *Macromolecules* **2007**, *40*, 3223–3228.
- (17) Fragiadakis, D.; Dou, S.; Colby, R. H.; Runt, J. *J. Chem. Phys.* **2009**, *130*, 064907.
- (18) Teeters, D.; Frech, R. *Solid State Ionics* **1986**, *18*, 271–276.
- (19) Kakihana, M.; Schantz, S.; Torell, L. M. *J. Chem. Phys.* **1990**, *92*, 6271–6277.
- (20) Schantz, S.; Torell, L. M.; Stevens, J. R. *J. Chem. Phys.* **1991**, *94*, 6862–6867.
- (21) Schantz, S. *J. Chem. Phys.* **1991**, *94*, 6296–6306.
- (22) Bastek, J.; Stolwijk, N. A.; Köster, T. K.-J.; van Wüllen, L. *Electrochim. Acta* **2010**, *55*, 1289–1297.
- (23) Lu, X.; Weiss, R. A. *Macromolecules* **1995**, *28*, 3022–3029.
- (24) Wintersgill, M. C.; Fontanella, J. J.; Greenbaum, S. G.; Adamić, K. J. *Br. Polym. J.* **1988**, *20*, 195–198.
- (25) Benetatos, N. M.; Heiney, P. A.; Winey, K. I. *Macromolecules* **2006**, *39*, 5174–5176.
- (26) Yarusso, D. J.; Cooper, S. L. *Polymer* **1985**, *26*, 371–378.
- (27) Yarusso, D. J.; Cooper, S. L. *Macromolecules* **1983**, *16*, 1871–1880.
- (28) MacKnight, W. J.; Taggart, W. P.; Stein, R. S. *J. Polym. Sci. Part C-Polym. Symp.* **1974**, *45*, 113–128.
- (29) Marx, C. L.; Caulfield, D. F.; Cooper, S. L. *Macromolecules* **1973**, *6*, 344–353.
- (30) Delf, B. W.; MacKnight, W. J. *Macromolecules* **1969**, *2*, 309–310.
- (31) Williams, C. E.; Russell, T. P.; Jerome, R.; Horrión, J. *Macromolecules* **1986**, *19*, 2877–2884.
- (32) Ding, Y. S.; Register, R. A.; Yang, C. Z.; Cooper, S. L. *Polymer* **1989**, *30*, 1213–1220.
- (33) Tomita, H.; Register, R. A. *Macromolecules* **1993**, *26*, 2791–2795.
- (34) Klein, R. J.; Zhang, S. H.; Dou, S.; Jones, B. H.; Colby, R. H.; Runt, J. *J. Chem. Phys.* **2006**, *124*, 144903.